

# Three-Dimensional Finite Element Analysis of Free Fibular Flap Reconstruction of Mandible Defects

Y Sun, Y Guo, J Li\*, D Yang and K Hu

Department of Oral and maxillofacial surgery; the First Affiliated Hospital of Bengbu Medical College, Bengbu, Anhui Province 233004, China



\*Corresponding author: J Li, Department of Plastic Surgery, The First Affiliated Hospital of Bengbu Medical College, 287 Changhuai Road, Bengbu, Anhui, 233000, China

## ARTICLE INFO

Received: 📅 June 01, 2021

Published: 📅 June 07, 2021

**Citation:** Y Sun, Y Guo, J Li, D Yang, K Hu. Three-Dimensional Finite Element Analysis of Free Fibular Flap Reconstruction of Mandible Defects. Biomed J Sci & Tech Res 36(2)-2021. BJSTR. MS.ID.005831.

**Keywords:** Mandible Defect; Reconstruction of the Mandible

## ABSTRACT

The aim of this study was to establish finite element models of free fibular flap reconstruction of different types of mandibular defects. The finite models was created from CT image. The finite element method was used to carry out biological analysis. Comparative analysis of the stress distribution characteristics and the displacement changes in mandible were carried out. From the stress distribution nephogram, it could be concluded that the stress was mainly concentrated in the bilateral condylar neck, the anterior and posterior edges of the mandibular ramus, and the joint between the posterior end of the fibula and the mandible. The more mandibular defects that were present, the greater the corresponding stress on the contralateral condyle. Displacement nephogram: the inward displacement of the condyle on the affected side of a type B defect was more obvious than that of the normal mandible, and the most obvious in the X-axis direction, with a displacement of 1.61 mm; the BSS defect crossed the midline, and the bilateral condyles shifted inward causing posterior displacement; the displacement results of RBS and CRBS defects showed whether the condyle was involved in the bone defect, and the displacement changes after reconstruction were not significantly different. After mandibular reconstruction, the loss of attachment muscles can cause postoperative condylar displacement, resulting in postoperative occlusal disorder, opening deviation and other complications.

## Introduction

The mandible, as a movable bony scaffold underlying the lower 1/3 of the face, not only maintains the facial contour, but also is closely related to the functions of chewing, breathing and swallowing. In radical surgery for mandibular tumors, a large number of muscles attached to the mandible are stripped, resulting in a lack of coordination of the chewing muscles, resulting in complications such as limited mouth opening, jaw deviation, joint clicking and disorder of occlusal relationship [1-3]. In the past, the most commonly-used repair methods were titanium plate and personalized prosthesis, which are prone to complications such as titanium plate exposure and fracture after long-term observation. Therefore, it was gradually replaced by free iliac or rib grafts [4,5]. In 1989, Hidalgo first applied a free fibular flap for jaw defect repair [6]. Since then, the vascularized fibular flap has become the

most important method of mandibular defect repair because it has sufficient bone length, is easy to shape, as well as having fewer donor site complications and other advantages [7-9]. In recent years, with the development of digital technology, the accuracy of mandibular reconstruction is the common goal pursued by oral and maxillofacial surgeons [10-12]. Analysis of the shape and position of the mandible after reconstruction is not only conducive to optimizing the reconstruction plan, but also conducive to the analysis of factors affecting accuracy, improving clinical treatment effects, and reducing postoperative complications. To date, there have still been few biomechanical studies on the reconstruction of mandibular defects with fibula flaps. The Finite Element Method (FEM) is a mathematical simulation method for mechanical analysis. It is widely used for biomechanical analyses of complex structures with different shapes, loads and materials [13-15].

## Materials and Methods

### Modeling Materials

From the CT database, the mandible and fibula were scanned with a thickness of 0.625 mm. The scanning range was from the condyle to the submental point. The left leg was scanned from knee to ankle. Imaging data were obtained and saved in DICOM format.

### Establishment of Finite Element Models

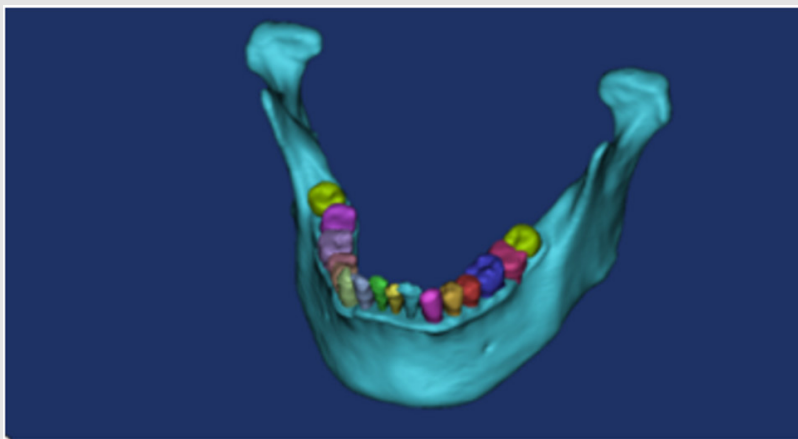


Figure 1: 3D model of the mandible.

The CT scan image was imported into Mimics 19.0 software. Adjusted the image gray value to generate a 3D model (Figure 1). Three points were selected on the surface of the mandible to establish a reference plane, and this was then used to draw a sketch to segment and simulate the mandibular defect. According to the clinical size of the titanium plate, the model was established and saved in the SLDPRT format. In the geometry, the mandibular cortical bone, mandibular cancellous bone, fibula, teeth, titanium

### Classification Standard of Mandible

According to the Urken classification [16], we established four types of mandibular defects, comprising type B (unilateral mandibular body defect), type BSS (bilateral mandibular body defect, crossing the midline), type RBS (unilateral mandibular body defect) and type CRBS (missing one side of the mandible).

plates and titanium nails were given relevant materials. In order to ensure the accuracy of the calculation, the type and size of the model grid was controlled, and the contact position grid was refined. The grid type was set to a 10-node tetrahedral grid. The boundary conditions and loads were set. Finally, three-dimensional finite element models of the normal mandible and four types of defects were established.

### Material Parameter Setting

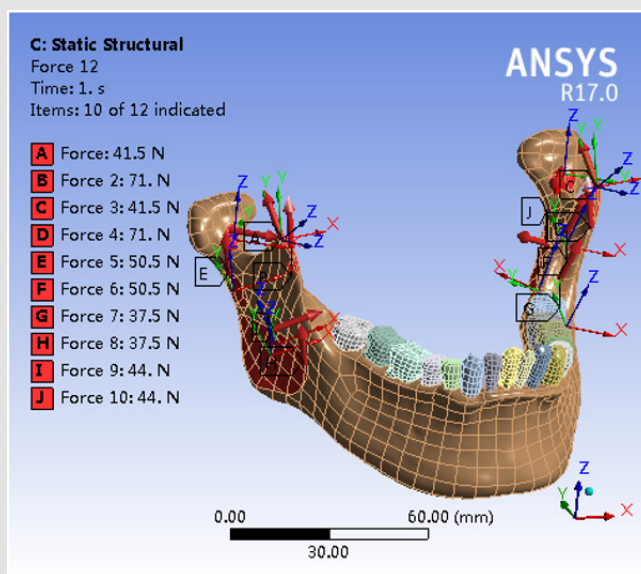


Figure 2: Masticatory muscle loading.

It was assumed that the mandible, teeth, fibula and other tissues are isotropic, homogeneous and continuous elastic materials. With reference to some published research data [17-19], the modulus of elasticity and Poisson's ratio were set. The mandibular condyles on both sides were fixed and restrained to prevent the mandible from moving, and the characteristics of the stress distribution of the mandible were analyzed. The chin was also fixed and the changes in the displacement of the mandible and condyle were analyzed. Vertical combined loading was applied on the healthy side posterior area by applying 200 N and 175 N to the mandibular first and second molar areas, respectively [20]. The medial pterygoid was loaded with 44 N, the deep and superficial layers of the masseter were loaded with 50.5 N and 37.5 N, respectively; the posterior and anterior portions of the temporalis were loaded with 41.5 N and 71 N, respectively, and the lateral pterygoid muscle was loaded with 5.5 N (Figure 2) [21,22].

### Internal Fixation Mode

The mandible and fibula were fixed with titanium plates. The width of the titanium plate was 7 mm, the thickness was 2 mm, and the hole diameter was 3.7 mm. Fixation was adjusted according to the shape of the bone surface.

### Main Observation Indicators

1. Stress distribution characteristics of the mandible
2. The displacement changes of the mandible on the x, y, and z axes. The x, y, and z axes represent the inside and outside, front and back, and up and down directions, respectively.

## Results

### Stress Distribution (Table 1)

1. The stress of the normal mandible was mainly concentrated on the neck of the bilateral condyles, the front and back edges of the mandibular ramus, and the joint between the posterior end of the fibula and the mandible. The maximum stress was approximately 47.29 MPa at the neck of the condyle.
2. In type B, the stress of the contralateral condyle was significantly greater than that of the affected condyle or the normal mandible by approximately 61.14 MPa.
3. In the BSS type, the stress concentration of bilateral condyles was similar, with stress values of 58.05 MPa and 51.61

MPa, respectively, both of which were higher than that of the normal mandible, but less than the maximum stress value of the B type defect.

4. In the RBS type, stress was mainly concentrated on the neck of the bilateral condyles, the joint of the fibula stump and the condyle. The maximum stress of the contralateral condyle was at the condyle of the affected side, with a value of approximately 86.14 MPa, which is close to twice the stress on the neck of the normal mandibular condyle.

5. In the CRBS type, the ipsilateral fibula was in a free state. The stress of the contralateral condyle was significantly greater than that of other types and normal mandibles, being three times that of the normal mandible.

**Table 1:** Stress distribution characteristics of mandible.

Objection	Maximum stress distribution of mandible (MPa)
normal	47.297
Type B	61.142
Type BSS	58.051
Type RBS	86.139
Type CRBS	116.84

### The Displacement Changes (Table 2)

The following results were obtained by finite element simulation analysis and calculation of the mandible:

1. The overall displacement of the normal intact mandible was 0.53 mm, consisting of 0.36 mm, 0.26 mm, and 0.45 mm on the X, Y, and Z axes, respectively.
2. The type B defect did not exceed the midline, the contralateral condyle shifted in the anterior and medial directions. The most obvious displacement was in the X-axis direction, approximately 1.61 mm.
3. The BSS-type defect crossed the midline, the displacement of the mandible was more obvious than others and the bilateral condyles were displaced inward and posteriorly.
4. In the RBS type and CRBS type, The partial or complete loss of the unilateral ascender muscle group caused the contralateral condyle to shift back and inward. There was no significant change in the displacement of the affected condyle.

**Table 2:** Displacement of normal mandible and each defect reconstructed with a fibular graft.

Objection	Total displacement (mm)	X direction displacement (mm)	Y direction displacement (mm)	Z direction displacement (mm)
Normal	0.52943	0.35673	0.25599	0.44909
Type B	2.2755	1.6102	0.35575	1.6673
Type BSS	3.5631	1.8747	1.3403	2.9134
Type RBS	0.34388	0.33025	0.092833	0.094739
Type CRBS	0.34551	0.3318	0.092252	0.095991

## Discussion

The repair of mandibular defects is one of the most difficult clinical problems in oral and maxillofacial surgery. In recent years, free fibular flap for reconstructing the mandible have gradually received attention [23-25].

The main reasons are as follows:

1. A free peroneal myocutaneous flap can provide sufficient bone mass. When the defect exceeds 9 cm, the fibula becomes the only option for reconstruction.
2. The anatomy of the perforating branches of the peroneal artery is relatively constant.
3. A skin island can be cut according to the needs of the defect, which can not only close the wound, but also can be used to observe the blood supply of the transplanted fibula.
4. The graft-harvesting operation is sited far away from the head and neck, allowing two groups of operations to be performed simultaneously. With the continuous accumulation of clinical experience, the purpose of mandibular reconstruction is not limited to restoring the continuity of the mandible and facial contours, but to further restore the patient's functions such as chewing, speech, and swallowing.

FEM is a powerful tool for biomechanical analysis, because it can provide a high degree of simulation of bone tissue biomechanics [26,27]. The geometric similarity between the finite element model of the mandible and the real mandible is the basis of the study, and directly affects the accuracy of data analysis [28,29]. In this study we established 3D models of fibula repair for type B, BSS, RBS, and RBSC defects. Different bone defects are accompanied by partial or full muscle defects, which affect the postoperative mandibular stress distribution and the mandibular shape and position. The main ascender muscle groups involved in mandibular movement include the temporalis (10.62 cm<sup>2</sup>), masseter (7.99 cm<sup>2</sup>), and medial pterygoid. The physiological cross-sectional area of masticatory muscles is positively correlated with muscle strength. Therefore, the temporal and masseter muscles have the greater muscle strength. Type B removes part of the masseter muscle attached to the corresponding position of the bone defect. Our results showed that the inward displacement of the affected mandible was significantly larger than that of the normal mandible,

while the displacement in other directions was not significantly different from that of the normal mandible. This shows that when the masseter contracts, it exerts an outward force on the mandible during the movement of the mandible. The BSS type defect crosses the midline, and the overall displacement is larger than that of the normal mandible or other defect types. The bilateral condyles are shifted inward, and the width of the dental arch becomes narrow. Since the bilateral defects in this study cross the midline and are symmetrical, the stress distribution and displacement changes were also more symmetrical than other types. The bilateral condyles shifted inward, and the width of the dental arch became narrow.

In the vertical direction, the mandible shifts up significantly. This study did not include the mylohyoid muscles or other lower mandibular jaw muscles. In fact, this type of defect is accompanied by the loss of their attachment at the same time as the bone defect, and the overall upward displacement should be greater. In the RBSC type, the mandibular ramus and condylar process are completely removed on one side. After reconstruction, the mandible is in the state of unilateral disconnection. Therefore, only the stress and displacement of the contralateral condyle can be measured. Comparing RBS-type and CRBS-type displacement distribution clouds, whether the condyle is retained or not has little effect on mandibular displacement. With more of the mandible missing on one side, the overall upward displacement of the mandible is significantly reduced. Both types of defects shifted significantly to the affected side. These changes are caused by the imbalance of bilateral muscle strength, which is also one of the important reasons for postoperative opening deflection. In the vertical direction, type B and BSS defects have a smaller displacement range than type RBS or CRBS, which is related to the suspension of the mandible by the ascender muscle group.

The results of a large number of clinical follow-up cases suggest that in cases where the coracoid process and the front edge of the mandibular ramus are not retained, the postoperative restriction of mouth opening will be reduced. During the clinical operation, the lesions do not involve the coracoid process. It is also considered to cut off the coracoid process and release the attachment of the temporal muscle to reduce postoperative complications. The maximum stress of the mandible model after reconstruction of various defects using a fibular graft is significantly greater than

that of the normal mandible. This shows that the original stress trajectory of the mandible is not restored after reconstruction, which results in an uneven stress distribution in the mandible. With the increase of the defect area of the affected mandible, the stress of the contralateral condyle also increases.

## Conclusion

The use of the FEM reduces the clinical dependence on a large number of cadavers and animal experiments. The theory is connected with the clinical practice, and the data provide certain guiding significance for the prevention and treatment of complications after reconstruction. The result of any finite element analysis is an approximation of the actual situation, with certain errors. Therefore, it is necessary to combine animal experiments and clinical observations with the FEM, so that all play a complementary role to achieve a comprehensive analysis.

## Conflict of Interest

We have no conflicts of interest.

## References

1. Genden EM (2010) Reconstruction of the mandible and the maxilla: the evolution of surgical technique. *Arch Facial Plast Surg* 12(2): 87-90.
2. Batstone MD (2018) Reconstruction of major defects of the jaws. *Aust Dent J* 63: S108-S113.
3. Wang W, Zhu J, Xu B, Xia B, Liu Y, et al. (2019) Reconstruction of mandibular defects using vascularized fibular osteomyocutaneous flap combined with nonvascularized fibular flap. *Medicina oral, patologia oral y cirugia bucal* 24(5): e691-e697.
4. Zhang Q, Wu W, Qian C, Xiao W, Zhu H, et al. (2019) Advanced biomaterials for repairing and reconstruction of mandibular defects. *Mater Sci Eng C Mater Biol Appl* 103: 109858.
5. Harashina T, Nakajima H, Imai T (1978) Reconstruction of mandibular defects with revascularized free rib grafts. *Plast Reconstr Surg* 62(4): 514-522.
6. Hidalgo DA (1989) Fibula free flap: a new method of mandible reconstruction. *Plast Reconstr Surg* 84(1): 71-79.
7. Patel A, Harrison P, Cheng A, Bray B, Bell RB (2019) Fibular Reconstruction of the Maxilla and Mandible with Immediate Implant-Supported Prosthetic Rehabilitation: Jaw in a Day. *Oral Maxillofac Surg Clin North Am* 31(3): 369-386.
8. Gonzalez SR, Hobbs B, Vural E, Moreno MA (2019) Functional outcome predictors following mandibular reconstruction with osteocutaneous fibula free flaps: correlating early postoperative videofluoroscopic swallow studies with long-term clinical results. *Maxillofac Plast Reconstr Surg* 41(1): 30.
9. Okay D, Al Shetawi AH, Moubayed SP, Mourad M, Buchbinder D, et al. (2016) Worldwide 10-Year Systematic Review of Treatment Trends in Fibula Free Flap for Mandibular Reconstruction. *J Oral Maxillofac Surg* 74(12): 2526-2531.
10. Nobis CP, Kesting MR, Wolff KD, Frohwitter G, Rau A, et al. (2020) Development of a template tool for facilitating fibula osteotomy in reconstruction of mandibular defects by digital analysis of the human mandible. *Clin Oral Investig* 24(9): 3077-3083.
11. Saini V, Gaba S, Sharma S, Kalra P, Sharma RK (2019) Assessing the Role of Virtual Surgical Planning in Mandibular Reconstruction With Free Fibula Osteocutaneous Graft. *J Craniofac Surg* 30(6): e563-e566.
12. Chang EI, Boukvalas S, Liu J, Largo RD, Hanasono MM, et al. (2019) Reconstruction of Posterior Mandibulectomy Defects in the Modern Era of Virtual Planning and Three-Dimensional Modeling. *Plast Reconstr Surg* 144(3): 453e-462e.
13. Cheng KJ, Liu YF, Wang JH, Jun C, iang XF, et al. (2019) Biomechanical behavior of mandibles reconstructed with fibular grafts at different vertical positions using finite element method. *J Plast Reconstr Aesthet Surg* 72(2): 281-289.
14. Kober C, Hellmich C, Gurin A, Komlev VS, Kjeller G, et al. (2017) Pathological mandibular biomechanics: finite element analysis based on partial dentition, cystic lesion, and partial resection[J]. *International Journal of Computer Assisted Radiology and Surgery* 12(1): 253.
15. Singh P, Wang C, Ajmera DH, Xiao SS, Song J, et al. (2016) Biomechanical Effects of Novel Osteotomy Approaches on Mandibular Expansion: A Three-Dimensional Finite Element Analysis. *J Oral Maxillofac Surg* 74(8): 1658.e1-1658.e15.
16. Urken ML, Buchbinder D, Weinberg H, Vickery C, Sheiner A, et al. (2015) Functional evaluation following microvascular oromandibular reconstruction of the oral cancer patient: A comparative study of reconstructed and nonreconstructed patients. *Laryngoscope* 125(7): 1512.
17. Styranivska O, Kliuchkovska N, Mykyeyevych N (2017) Comparison of using different bridge prosthetic designs for partial defect restoration through mathematical modeling. *Eur J Dent* 11(3): 345-351.
18. Murakami K, Yamamoto K, Sugiura T, Horita S, Matsusue Y, et al. (2017) Computed Tomography-Based 3-Dimensional Finite Element Analyses of Various Types of Plates Placed for a Virtually Reduced Unilateral Condylar Fracture of the Mandible of a Patient. *J Oral Maxillofac Surg* 75(6): 1239.e1-1239.e11.
19. Kumar D, Sivaram G, Shivakumar B, Kumar Tss (2018) Comparative evaluation of soft and hard tissue changes following endosseous implant placement using flap and flapless techniques in the posterior edentulous areas of the mandible-a randomized controlled trial. *Oral Maxillofac Surg* 22(2): 215-223.
20. Kanazawa M, Tanoue M, Miyayasu A, Takeshita S, Sato D, et al. (2018) The patient general satisfaction of mandibular single-implant overdentures and conventional complete dentures: Study protocol for a randomized crossover trial. *Medicine (Baltimore)* 97(20): e10721.
21. Koolstra JH, Van Eijden TM, Van Spronsen PH, Weijs WA, Valk J (1990) Computer-assisted estimation of lines of action of human masticatory muscles reconstructed *in vivo* by means of magnetic resonance imaging of parallel sections. *Arch Oral Biol* 35(7): 549-556.
22. Weijs WA, Hillen B (1984) Relationship between the physiological cross-section of the human jaw muscles and their cross-sectional area in computer tomograms. *Acta Anat (Basel)* 118(3): 129-138.
23. Li J, Song P, Yang D, Liu L, Wang J (2020) Complicated intraoral defects: reconstruction using a three-paddle perforator free flap. A case report. *Br J Oral Maxillofac Surg* 58(3): 355-357.
24. Batstone MD (2018) Reconstruction of major defects of the jaws. *Aust Dent J* 63: S108-S113.
25. Gallegos-Hernández JF, Martínez-Miramón A, Reyes-Vivanco A (2019) Fibular free flap in mandible reconstruction, a long-term follow-up. Seguimiento a largo plazo del colgajo libre de peroné en la reconstrucción mandibular. *Cir Cir* 87(3): 267-271.
26. Wong RC, Tideman H, Merckx MA, Jansen J, Goh SM, et al. (2011) Review of biomechanical models used in studying the biomechanics of reconstructed mandibles. *Int J Oral Maxillofac Surg* 40(4): 393-400.
27. Parr WC, Wroe S, Chamoli U, Richards HS, McCurry MR, et al. (2012) Toward integration of geometric morphometrics and computational biomechanics: new methods for 3D virtual reconstruction and quantitative analysis of Finite Element Models. *J Theor Biol* 301: 1-14.

28. Okumura N, Stegaroiu R, Nishiyama H, Kurokawa K, Kitamura E, et al. (2011) Finite element analysis of implant-embedded maxilla model from CT data: comparison with the conventional model. J Prosthodont Res 55(1): 24-31.
29. Orentlicher G, Goldsmith D, Horowitz A (2010) Applications of 3-dimensional virtual computerized tomography technology in oral and maxillofacial surgery: current therapy. J Oral Maxillofac Surg 68(8): 1933-1959.

ISSN: 2574-1241

DOI: 10.26717/BJSTR.2021.36.005831

J Li. Biomed J Sci & Tech Res



This work is licensed under Creative Commons Attribution 4.0 License

Submission Link: <https://biomedres.us/submit-manuscript.php>



#### Assets of Publishing with us

- Global archiving of articles
- Immediate, unrestricted online access
- Rigorous Peer Review Process
- Authors Retain Copyrights
- Unique DOI for all articles

<https://biomedres.us/>